

Published in final edited form as:

Mol Immunol. 2011 March ; 48(6-7): 973–978. doi:10.1016/j.molimm.2011.01.004.

p21 is dispensable for AID-mediated class switch recombination and mutagenesis of immunoglobulin genes during somatic hypermutation

Maryam Shansab and Erik Selsing*

Program in Immunology and Department of Pathology Sackler School of Graduate Biomedical Sciences Tufts University School of Medicine, Boston, Massachusetts, 02111, USA

Abstract

In B cells, activation-induced cytidine deaminase (AID) induces somatic hypermutation (SHM) at rearranged immunoglobulin (Ig) variable (V) regions. Previous studies have shown that both monoubiquitination of proliferating cell nuclear antigen (PCNA) and translesional DNA polymerase activity are important for inducing mutagenesis during SHM. Regulation of PCNA ubiquitination by p21, also known as Cdkn1a and p21^{Cip1/Waf1}, is an important mechanism that controls mutation loads in mammalian cells. In this study, we have assessed whether p21 has an *in vivo* function in regulating mutagenesis in B cells by analyzing SHM frequency in p21 deficient mice. Our results show that p21 is dispensable for SHM. This suggests that, during SHM of Ig genes, p21 does not act to regulate mutagenesis load. We also show that p21 transcript levels are the same in both wildtype and AID-deficient B cells during B cell activation, and that AID-mediated class switch recombination (CSR) is not affected by p21-deficiency; thereby indicating that p21 regulation in B cells is not altered by AID-induced DNA damage and that p21 has no affect on AID-dependent Ig gene diversification. Our results suggest that regulation of p21 in activated B cells is probably more important for maintaining proper cell cycle progression as opposed to promoting SHM of Ig genes.

Keywords

Somatic hypermutation; CDKN1A; p21^{Cip1/Waf1}; Proliferating cell nuclear antigen; Translesional DNA polymerases; Immunoglobulin variable genes

1. Introduction

SHM is a process that introduces point mutations into recombined Ig V regions during B cell activation and, thereby, leads to selected increases in the affinity of antibodies (Ab) during responses to pathogens. The rate of SHM is about 1 mutation per 1000 base pairs (bp) per cell cycle, which is close to a million fold higher than the spontaneous mutation rate that occurs in the remainder of the genome (Kunkel, 2004; Rajewsky, 1996). Although

*corresponding author, Correspondence to: Erik Selsing, 150 Harrison Ave, Jaharis Bldg. Rm 512, Boston, MA 02111, Telephone: 617-636-0467, Fax: 617-636-2990, Erik.Selsing@tufts.edu.

Publisher's Disclaimer: This is a PDF file of an unedited manuscript that has been accepted for publication. As a service to our customers we are providing this early version of the manuscript. The manuscript will undergo copyediting, typesetting, and review of the resulting proof before it is published in its final citable form. Please note that during the production process errors may be discovered which could affect the content, and all legal disclaimers that apply to the journal pertain.

mechanisms and regulation of SHM are not fully understood, key aspects of the pathway have been characterized (Peled et al., 2008).

SHM is initiated by the enzyme AID (Muramatsu et al., 2000) which deaminates cytosine residues to uracils on single stranded DNA (ssDNA) leading to the formation of U:G bp mismatches (Bransteitter et al., 2003; Dickerson et al., 2003; Petersen-Mahrt et al., 2002). Mutations are generated upon processing/removing the uracils from the DNA by several DNA repair pathways. The base excision repair (BER) and mismatch repair (MMR) pathways play important roles in processing of the U:G bp mismatches (Rada et al., 2004; Shen et al., 2006). Removal of uracils by uracil-DNA glycosylase (UNG), which is part of the BER pathway, results in abasic sites that can be repaired by replication via error-prone polymerases to produce both transition mutations (purine to purine or pyrimidine to pyrimidine) and transversion mutations (purine to pyrimidine) at the original C:G bp (Rada et al., 2002). As part of the MMR pathway, the Msh2 and Msh6 heterodimers can also recognize the U:G bp mismatches and initiate the removal of the uracils by DNA excision followed by resynthesis via error-prone polymerases which can produce mutations at base pairs surrounding the original C:G site that was deaminated by AID (Rada et al., 1998; Wiesendanger et al., 2000; Wilson et al., 2005). Low fidelity, error-prone, translesional DNA polymerases such as Pol η , θ , ι , ζ , and REV1 have been shown to be important for SHM (Delbos et al., 2007; Delbos et al., 2005; Diaz et al., 2001; Faili et al., 2002; Jansen et al., 2006; Masuda et al., 2005; Mayorov et al., 2005; McDonald et al., 2003; Ross and Sale, 2006; Schenten et al., 2009; Zan et al., 2001; Zeng et al., 2001).

The DNA repair pathways that are functional during SHM are also essential in protecting the genome from deleterious mutagenesis. For example, Ung and Msh2/Msh6 play important roles in repairing spontaneous DNA damage that occurs during DNA replication (Barnes and Lindahl, 2004; Kavli et al., 2007). Furthermore, Ung and Msh2 are essential for the error-free repair of AID-induced DNA damage that occurs in non-Ig genes during B cell activation (Liu et al., 2008). There is little known about the mechanisms that regulate error-free versus error-prone mechanisms of DNA repair pathways during SHM.

Recently, it has been shown that monoubiquitination of the DNA clamp PCNA is important for SHM (Langerak et al., 2007; Roa et al., 2008). PCNA is a ring shaped homotrimer that is essential in DNA replication and DNA repair (Moldovan et al., 2007). Monoubiquitination of PCNA regulates the loading and unloading of error-prone versus error-free DNA polymerases (Kannouche et al., 2004; Stelter and Ulrich, 2003; Watanabe et al., 2004). Studies from mice that express a mutated form of PCNA which cannot be monoubiquitinated show a drastic reduction of mutations at A:T bp during SHM (Langerak et al., 2007; Roa et al., 2008). Furthermore, defects of PCNA monoubiquitination result in decrease SHM in the DT40 chicken B cell lines (Arakawa et al., 2006). These results indicate that ubiquitination status of PCNA during SHM may regulate the choice between error-free versus error-prone DNA repair pathways.

The regulatory mechanisms that promote error-prone repair by monoubiquitination of PCNA post AID-induced DNA damage are not yet known. Several studies in human cell lines have shown that the tumor suppressor protein p53 and the cell cycle inhibitor protein p21 control mutation loads by affecting PCNA ubiquitination (Avkin et al., 2006; Soria et al., 2006). Furthermore, loss of p53 and/or p21 results in uncontrolled error-prone translesional polymerase activity (Avkin et al., 2006). Because p21 binds PCNA near the vicinity of the ubiquitination site, it has been suggested that p21 binding to PCNA may impair the function of PCNA to switch to a lower fidelity DNA polymerase such as pol η (Gulbis et al., 1996; Kannouche et al., 2004; Soria et al., 2006; Soria et al., 2008; Watanabe et al., 2004).

The role of p21 in B cells is not clear. Studies have suggested that inactivating p21 during B cell activation may be essential to allow proper cell cycle progression (Phan et al., 2005; Woo et al., 2003). However, because p21 can also function as a negative regulator of mutagenesis by modulating PCNA ubiquitination, it is unclear whether p21 inactivation in B cells is essential for promoting SHM or preventing cell cycle arrest. We have now investigated the role of p21 during SHM. We tested whether p21 deficient (*Cdkn1a*^{-/-}) B cells displayed alterations in SHM, specifically increases in mutations at A:T bp which would be predicted if p21 functioned as a negative regulator of error-prone translesional polymerases. Furthermore, we have tested whether p21 regulation during B cell activation was dependent on AID-induced DNA damage.

2. Materials and Methods

2.1. Mice

All experiments with mice were approved by and performed in accordance with the regulations of the Tufts University School of Medicine IACUC. Mice deficient in p21 (*Cdkn1a*^{-/-}) have been described elsewhere (Brugarolas et al., 1995), are phenotypically normal up to 7 months of age (Balomenos et al., 2000), and were obtained from Richard Van Etten (Tufts University School of Medicine, Boston, Massachusetts). The AID-deficient (*Aicda*^{-/-}) mice were obtained from Thereza Imanishi-Kari (Tufts University School of Medicine, Boston, Massachusetts) with permission from T. Honjo (Kyoto University, Kyoto, Japan) and have also been described elsewhere (Muramatsu et al., 2000). All mice were maintained in a pathogen-free mouse facility at Tufts University School of Medicine.

2.2. Quantitative Real-time PCR

B cells were isolated from splenocytes of 3 *Aicda*^{-/-} mice and 2 *Aicda*^{+/+} mice (2 months old) by negative selection using B cell isolation kits (Stem Cell Tech). Two million B cells were stimulated for 8hr, 24hr, 48hr, 72hr, and 96hr with 25µg/ml of LPS (Sigma) and 10ng/ml of IL-4 (Pepro Tech) in 4 ml cultures consisting of RPMI-1640 (BioWhittaker) supplemented with 10% FBS (Atlanta Biologicals). Unstimulated cells (time 0hr) were lysed in TRIzol (Invitrogen) after B cell isolation. Total RNA was isolated with TRIzol following the manufacturer's protocol (Invitrogen). The RNA was DNaseI (Invitrogen) treated prior to cDNA synthesis. One microgram of RNA was used for cDNA synthesis using oligo(dT)20 and SuperScript III as recommended by the manufacturer (Invitrogen). Real-time PCR was performed with SYBR® Green PCR master mix (Applied Biosystems) with mouse p21 primers (forward- 5' CACAGGCACCATGTCCAATC, and reverse- 5' GACAACGGCACACTTTGCTC) and mouse β-actin primers (for endogenous control) (forward- 5' AGGTATCCTGACCCTGAAC, and reverse- 5' CACACGCAGCTCATTGTAG) in a IQ™5 Multicolor Real-Time PCR Detection System (Bio-Rad). WEHI-231 murine B-cell lines were used to make standard curves for p21 and β-actin expression. Relative quantification was determined from the standard curves and by normalizing to β-actin. Real-Time PCR data represent the means that were obtained from triplicates from three independent experiments. Student's *t*-tests were performed to determine statistical differences.

2.3. Cell sorting

Cells were stained with the B cell marker, B220 (CD45R/B220-PE, Southern Biotech), and the activation marker, peanut agglutinin (PNA) (FITC-PNA, Vector Laboratories Inc.) by standard methods. Activated B cells were isolated by sorting for B220⁺PNA^{high} on a MoFlo instrument (Dako Cytomation), and FACS analysis was done with FACSCalibur (BD Biosciences).

2.4. SHM

Activated B cells were sorted from Peyer's patches of 2–4 month old *Cdkn1a*^{-/-} mice (4 mice per experiment, a total of three independent experiments), *Cdkn1a*^{+/+} littermate controls (4 mice per experiment, a total of 2 independent experiments) and *Cdkn1a*^{+/-} littermate controls (4 mice in one experiment). Activated B cells (B220⁺PNA^{high}) were sorted and lysed for DNA isolation using Aqua Pure Genomic DNA isolation kits (Bio-Rad). The Jh2 to Jh4 intronic region (~1.4 kilobases) of the Ig locus was amplified using the Jh2-forward primer; 5' GGCACCACTCTCACAGTCTCCTCAGG and Jh4-reverse primer; 5' TGAGACCGAGGCTAGATGCC. High fidelity *Pfx Platinum Taq DNA Polymerase* was used for the amplification process as described by the manufacturer (Invitrogen). The PCR error rate was 2.2×10^{-4} which was determined from sorted naïve B cells (B220⁺PNA^{low/-}). The PCR products were separated on an agarose gel and the 1.4 kb products were isolated from the gel using QIAquick Gel Extraction kits (Qiagen). Gel purified PCR products were cloned into pGEM vectors (Promega) and transformed into 5-alpha F' *I*⁹competent *Escherichia coli* (New England BioLabs). Plasmids containing individual PCR clones were isolated as described before (Han et al., 2007). Each clone was sequenced bidirectionally with two different primers (T7 and Sp6) that hybridize to the pGEM vector (Promega). Sequencing was performed at the Tufts University Core Facility (Tufts University School of Medicine, Boston, MA). The sequences were analyzed with Clone Manager software (Sci-ED) and SHM was determined by dividing the total number of mutations that were observed by the total number of bp that were analyzed. Clones that contained identical mutations, and clones that shared some mutations, were counted once. In our analysis, only 2 clones shared mutations, one clone had 15 mutations that were identical to the sister clone which had 5 additional mutations; of these, only the clone with the most mutations was included in the analysis. Among the identical clones, 5 set of clones (10 total clones) contained identical mutations and each set was counted as one clone. The sequence specificity data only includes clones that were counted in the pie charts. Both the mutation frequency and the mutation patterns were confirmed by the SHMTool webserver (<http://scb.aecom.yu.edu/cgi-bin/p1>) (Maccarthy et al., 2009) and corrected for base composition. *P* values were calculated using two-tailed unpaired Student's *t*-tests.

2.5. CSR

B cells were isolated from splenocytes of 3 *Cdkn1a*^{-/-} mice and 3 *Cdkn1a*^{+/+} controls by negative selection using B cell isolation kits (Stem Cell Tech). Two million B cells were activated for four days to induce CSR to IgG1 (25µg/ml LPS + 20ng/ml IL-4), IgG3 (25µg/ml LPS), IgG2a (25µg/ml LPS + 100ng/ml IFN-γ), IgG2b (25µg/ml LPS + 0.5ng/ml TGF-β) as described elsewhere (Eccleston et al., 2009). Four days post stimulation, B cells were stained with Alexa Fluor®467-conjugated anti-B220 (Invitrogen), and either with Alexa Fluor®488-conjugated anti-IgG1, anti-IgG3, anti-IgG2a, or anti-IgG2b (Invitrogen). Propidium iodide (PI) was added just prior to FACS analysis with FACSCalibur (BD Biosciences). Three independent experiments (one mouse per genotype per experiment) were conducted and the *p* values were calculated using two-tailed unpaired Student's *t*-tests.

3. Results

3.1. p21 expression is not regulated by AID

We first examined the expression pattern of p21 during B cell activation, and also assessed whether AID expression affected the p21 expression pattern, by performing a time-course experiment to monitor p21 mRNA levels at different time points. B cells from wildtype (*Aicda*^{+/+}) or AID-deficient (*Aicda*^{-/-}) mice were either unstimulated or stimulated with LPS and IL-4 for 8, 24, 48, 72, or 96 hours (hr), and then p21 mRNA levels were determined by quantitative Real-time PCR. As shown in Fig. 1, p21 mRNA levels sharply

increase 50–65 fold at 8 hours after B cell stimulation and then, drop to near unstimulated levels at 24 hours post stimulation. Subsequently, p21 expression increases to 13–18 fold at 48 and 72 hours post stimulation, reaching a maximum of 25 fold at 96 hours post stimulation. We did not detect any significant difference in p21 expression levels between *Aicda*^{+/+} and *Aicda*^{-/-} B cells. These data indicate that the pattern of p21 expression levels in stimulated B cells are regulated independent of AID.

3.2. p21 is dispensable for SHM

To investigate whether p21 deficiency had a significant effect on SHM frequency, we isolated activated B cells from Peyer's patches of *Cdkn1a*^{-/-} mice and *Cdkn1a*^{+/+} or *Cdkn1a*^{+/-} littermate controls. Because the results from *Cdkn1a*^{+/+} and *Cdkn1a*^{+/-} mice were similar (Supp. Table 1) we pooled them and refer to these as wildtype in these SHM experiments. Activated B cells from Peyer's patches are activated naturally by gut-associated antigens (Gonzalez-Fernandez and Milstein, 1993) and activated B cells were isolated as B220⁺PNA^{high}. To assess Ig locus SHM, DNAs containing the Jh2-Jh4 intronic region of the Ig locus were amplified to monitor mutations that are not located in coding regions and, therefore, are not affected by antigenic selection. A total of 115 clones from wildtype mice and a total of 99 clones from *Cdkn1a*^{-/-} mice were analyzed for SHM by sequence analyses. We found no differences in SHM frequency or in mutation patterns when comparing *Cdkn1a*^{-/-} and wildtype mice (Fig. 2). The mutation frequency in *Cdkn1a*^{-/-} mice (2.77×10^{-3}) was somewhat lower than in wildtype mice (3.21×10^{-3}), but this difference was not statistically significant (Fig. 2A, top). In addition, the percentage of mutated clones was similar between wildtype (56%) and *Cdkn1a*^{-/-} (54%) mice, indicating that p21 deficiency did not lead to an increase in the number of B cells undergoing SHM (Fig. 2A, bottom). Furthermore, the numbers of mutations per clone in *Cdkn1a*^{-/-} and wildtype B cells were similar; about 19% of the clones in the wildtype mice, and 17% of the clones in the *Cdkn1a*^{-/-} mice exhibited 7–40 mutations (Fig. 2A, bottom).

Our results also indicated that the SHM mutation pattern was the same in both wildtype and *Cdkn1a*^{-/-} mice (Fig. 2B). The frequency of mutations at each base (A, T, G, C) was not significantly altered in *Cdkn1a*^{-/-} mice (Fig 2C). About half of the mutations were transition mutations (wildtype 51.3%, *Cdkn1a*^{-/-} 49.9%) and the other half were transversion mutations (wildtype 48.7%, *Cdkn1a*^{-/-} 50.1%) (Table 1). Most importantly, mutations at A:T bp, which can be generated by translesional DNA pol η , were not affected by the absence of p21 (wildtype 62.8%, *Cdkn1a*^{-/-} 61.9%), and the percent of mutations at DNA pol η hotspots were not statistically different between the two mouse strains (Table 1).

In order to investigate whether p21 had a role in CSR, we tested the ability of *Cdkn1a*^{-/-} B cells to class switch to IgG1, IgG3, IgG2a, and IgG2b when stimulated *ex vivo*. The percentage of CSR in both wildtype and *Cdkn1a*^{-/-} B cells were similar (Fig. 3), indicating that, as with SHM, p21 does not function in CSR. Based on these data, we conclude that p21 does not play a role in regulating Ab gene diversification in B cells.

4. Discussion

Our results show that, in activated B cells, p21 deficiency does not alter the amount of AID-induced mutagenesis that occurs within the Igh locus during SHM and CSR. This contrasts with the known role of p21 (together with the tumor-suppressor protein, p53) in controlling DNA-damage-mediated mutagenesis in other types of mammalian cells (Avkin et al., 2006). Based on previous studies, it could be suggested that the lack of a p21 effect on SHM could result from a specific down-regulation of p21 in these cells (Phan et al., 2005; Woo et al., 2003). These studies, however, did not address the *in vivo* role of p21 in B cells, particularly whether downregulation of p21 might be a mechanism to promote SHM. We find that,

although p21 transcript levels do decrease in the period between 8 to 24 hours after B cell stimulation, these levels recover during the period 48 to 96 hours after stimulation, at the times when AID-induced DNA damage repair leads to CSR events (Rush et al., 2005). Furthermore, we show that the p21 expression pattern does not differ between wildtype and AID-deficient mice, indicating that regulation of p21 is independent of AID activity. We suspect that reduction of functional p21 expression may be relevant for cell cycle control as suggested previously (Phan et al., 2005; Woo et al., 2003), but not for SHM.

We also find that, at least for the Igh loci, which are poised to accrue mutations, p21 deficiency does not result in an increase in SHM as would be predicted if p21 had a negative regulatory role. Our results are consistent with the findings from a recent study that investigated the role of p53 and p21 in SHM (Ratnam et al., 2010). This study shows that the mutation spectrum is altered in p53 deficient B cells. This change, however, was not detected in B cells lacking p21 or in p53/Ung double deficient B cells (Ratnam et al., 2010). Based on these findings, it was concluded that p21 does not function in SHM. Perhaps it is more likely that p21 activity is excluded from the Igh locus during SHM and, therefore, p21 deletion has no effect on the frequency of Igh locus SHM. However, we do not know whether p21 expression might, at later time points, function to prevent mutagenesis at non-Ig genes that have also been shown to accumulate AID-induced DNA damage but that are repaired in an error-free manner (Liu et al., 2008). Indeed, it has been shown that p21 can interfere with PCNA ubiquitination and the ability of PCNA to load translesional DNA polymerases, such as Pol η , in human cell lines (Soria et al., 2006; Soria et al., 2008). Furthermore, PCNA mutants that are unable to become monoubiquitinated show discernable effects on SHM, particularly at bases that are targeted by Pol η (Langerak et al., 2007; Roa et al., 2008). Therefore, it is possible that p21 interaction with PCNA may promote error-free repair of non-Ig genes, but it is clear from our results that p21 does not affect the SHM process at the Igh loci.

Since p21 can function in promoting error-free DNA repair by regulating DNA polymerase loading onto PCNA (Soria et al., 2006; Soria et al., 2008), we also considered that the absence of p21 might result in the inhibition of faithful DNA repair of Ig switch regions and could create more double stranded DNA (dsDNA) breaks as reported for B cells lacking the error-free DNA polymerase Pol β (Schrader et al., 2009). Therefore, an increase in CSR might be anticipated in p21-deficient B cells. We tested this hypothesis and found that CSR is not affected in p21-deficient B cells, indicating that p21 does not play a role in AID-mediated Ig gene diversification.

Supplementary Material

Refer to Web version on PubMed Central for supplementary material.

Acknowledgments

This work was supported by a National Institutes of Health Grant (AI24465), by the Eshe Foundation, and by the W.M. Keck Foundation.

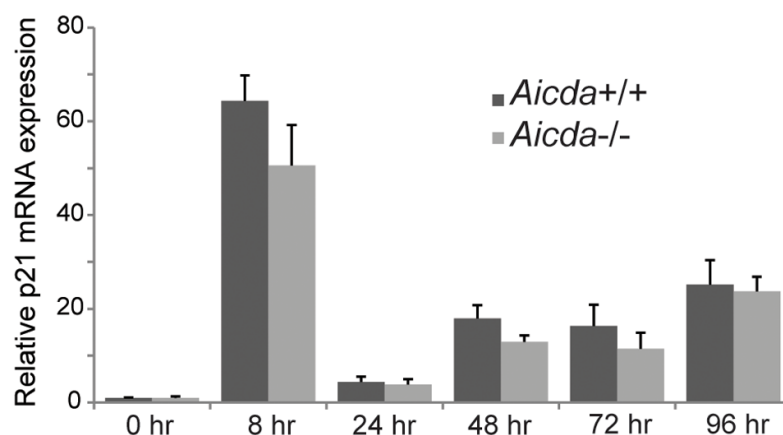
References

- Arakawa H, Moldovan GL, Saribasak H, Saribasak NN, Jentsch S, Buerstedde JM. A role for PCNA ubiquitination in immunoglobulin hypermutation. *PLoS Biol.* 2006; 4:e366. [PubMed: 17105346]
- Avkin S, Sevilya Z, Toube L, Geacintov N, Chaney SG, Oren M, Livneh Z. p53 and p21 regulate error-prone DNA repair to yield a lower mutation load. *Mol Cell.* 2006; 22:407–13. [PubMed: 16678112]

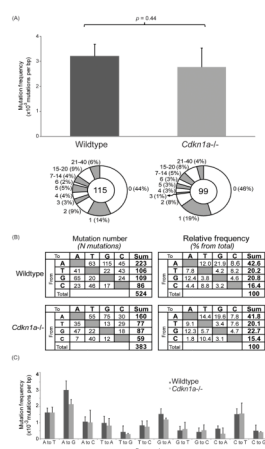
- Balomenos D, Martin-Caballero J, Garcia MI, Prieto I, Flores JM, Serrano M, Martinez AC. The cell cycle inhibitor p21 controls T-cell proliferation and sex-linked lupus development. *Nat Med*. 2000; 6:171–6. [PubMed: 10655105]
- Barnes DE, Lindahl T. Repair and genetic consequences of endogenous DNA base damage in mammalian cells. *Annu Rev Genet*. 2004; 38:445–76. [PubMed: 15568983]
- Bransteitter R, Pham P, Scharff MD, Goodman MF. Activation-induced cytidine deaminase deaminates deoxycytidine on single-stranded DNA but requires the action of RNase. *Proc Natl Acad Sci U S A*. 2003; 100:4102–7. [PubMed: 12651944]
- Brugarolas J, Chandrasekaran C, Gordon JI, Beach D, Jacks T, Hannon GJ. Radiation-induced cell cycle arrest compromised by p21 deficiency. *Nature*. 1995; 377:552–7. [PubMed: 7566157]
- Delbos F, Aoufouchi S, Faili A, Weill JC, Reynaud CA. DNA polymerase eta is the sole contributor of A/T modifications during immunoglobulin gene hypermutation in the mouse. *J Exp Med*. 2007; 204:17–23. [PubMed: 17190840]
- Delbos F, De Smet A, Faili A, Aoufouchi S, Weill JC, Reynaud CA. Contribution of DNA polymerase eta to immunoglobulin gene hypermutation in the mouse. *J Exp Med*. 2005; 201:1191–6. [PubMed: 15824086]
- Diaz M, Verkoczy LK, Flajnik MF, Klinman NR. Decreased frequency of somatic hypermutation and impaired affinity maturation but intact germinal center formation in mice expressing antisense RNA to DNA polymerase zeta. *J Immunol*. 2001; 167:327–35. [PubMed: 11418667]
- Dickerson SK, Market E, Besmer E, Papavasiliou FN. AID mediates hypermutation by deaminating single stranded DNA. *J Exp Med*. 2003; 197:1291–6. [PubMed: 12756266]
- Eccleston J, Schrader CE, Yuan K, Stavnezer J, Selsing E. Class switch recombination efficiency and junction microhomology patterns in Msh2-, Mlh1-, and Exo1-deficient mice depend on the presence of mu switch region tandem repeats. *J Immunol*. 2009; 183:1222–8. [PubMed: 19553545]
- Faili A, Aoufouchi S, Flatter E, Guenger Q, Reynaud CA, Weill JC. Induction of somatic hypermutation in immunoglobulin genes is dependent on DNA polymerase iota. *Nature*. 2002; 419:944–7. [PubMed: 12410315]
- Gonzalez-Fernandez A, Milstein C. Analysis of somatic hypermutation in mouse Peyer's patches using immunoglobulin kappa light-chain transgenes. *Proc Natl Acad Sci U S A*. 1993; 90:9862–6. [PubMed: 8234326]
- Gulbis JM, Kelman Z, Hurwitz J, O'Donnell M, Kuriyan J. Structure of the C-terminal region of p21(WAF1/CIP1) complexed with human PCNA. *Cell*. 1996; 87:297–306. [PubMed: 8861913]
- Han JH, Akira S, Calame K, Beutler B, Selsing E, Imanishi-Kari T. Class switch recombination and somatic hypermutation in early mouse B cells are mediated by B cell and Toll-like receptors. *Immunity*. 2007; 27:64–75. [PubMed: 17658280]
- Jansen JG, Langerak P, Tsaalbi-Shtylik A, van den Berk P, Jacobs H, de Wind N. Strand-biased defect in C/G transversions in hypermutating immunoglobulin genes in Rev1-deficient mice. *J Exp Med*. 2006; 203:319–23. [PubMed: 16476771]
- Kannouche PL, Wing J, Lehmann AR. Interaction of human DNA polymerase eta with monoubiquitinated PCNA: a possible mechanism for the polymerase switch in response to DNA damage. *Mol Cell*. 2004; 14:491–500. [PubMed: 15149598]
- Kavli B, Otterlei M, Slupphaug G, Krokan HE. Uracil in DNA--general mutagen, but normal intermediate in acquired immunity. *DNA Repair (Amst)*. 2007; 6:505–16. [PubMed: 17116429]
- Kunkel TA. DNA replication fidelity. *J Biol Chem*. 2004; 279:16895–8. [PubMed: 14988392]
- Langerak P, Nygren AO, Krijger PH, van den Berk PC, Jacobs H. A/T mutagenesis in hypermutated immunoglobulin genes strongly depends on PCNAK164 modification. *J Exp Med*. 2007; 204:1989–98. [PubMed: 17664295]
- Liu M, Duke JL, Richter DJ, Vinuesa CG, Goodnow CC, Kleinstein SH, Schatz DG. Two levels of protection for the B cell genome during somatic hypermutation. *Nature*. 2008; 451:841–5. [PubMed: 18273020]
- Maccarthy T, Roa S, Scharff MD, Bergman A. SHMTool: a webserver for comparative analysis of somatic hypermutation datasets. *DNA Repair (Amst)*. 2009; 8:137–41. [PubMed: 18952008]

- Masuda K, Ouchida R, Takeuchi A, Saito T, Koseki H, Kawamura K, Tagawa M, Tokuhisa T, Azuma TJOW. DNA polymerase theta contributes to the generation of C/G mutations during somatic hypermutation of Ig genes. *Proc Natl Acad Sci U S A*. 2005; 102:13986–91. [PubMed: 16172387]
- Mayorov VI, Rogozin IB, Adkison LR, Gearhart PJ. DNA polymerase eta contributes to strand bias of mutations of A versus T in immunoglobulin genes. *J Immunol*. 2005; 174:7781–6. [PubMed: 15944281]
- McDonald JP, Frank EG, Plosky BS, Rogozin IB, Masutani C, Hanaoka F, Woodgate R, Gearhart PJ. 129-derived strains of mice are deficient in DNA polymerase iota and have normal immunoglobulin hypermutation. *J Exp Med*. 2003; 198:635–43. [PubMed: 12925679]
- Moldovan GL, Pfander B, Jentsch S. PCNA, the maestro of the replication fork. *Cell*. 2007; 129:665–79. [PubMed: 17512402]
- Muramatsu M, Kinoshita K, Fagarasan S, Yamada S, Shinkai Y, Honjo T. Class switch recombination and hypermutation require activation-induced cytidine deaminase (AID), a potential RNA editing enzyme. *Cell*. 2000; 102:553–63. [PubMed: 11007474]
- Peled JU, Kuang FL, Iglesias-Ussel MD, Roa S, Kalis SL, Goodman MF, Scharff MD. The biochemistry of somatic hypermutation. *Annu Rev Immunol*. 2008; 26:481–511. [PubMed: 18304001]
- Petersen-Mahrt SK, Harris RS, Neuberger MS. AID mutates *E. coli* suggesting a DNA deamination mechanism for antibody diversification. *Nature*. 2002; 418:99–103. [PubMed: 12097915]
- Phan RT, Saito M, Basso K, Niu H, Dalla-Favera R. BCL6 interacts with the transcription factor Miz-1 to suppress the cyclin-dependent kinase inhibitor p21 and cell cycle arrest in germinal center B cells. *Nat Immunol*. 2005; 6:1054–60. [PubMed: 16142238]
- Rada C, Di Noia JM, Neuberger MS. Mismatch recognition and uracil excision provide complementary paths to both Ig switching and the A/T-focused phase of somatic mutation. *Mol Cell*. 2004; 16:163–71. [PubMed: 15494304]
- Rada C, Ehrenstein MR, Neuberger MS, Milstein C. Hot spot focusing of somatic hypermutation in MSH2-deficient mice suggests two stages of mutational targeting. *Immunity*. 1998; 9:135–41. [PubMed: 9697843]
- Rada C, Williams GT, Nilsen H, Barnes DE, Lindahl T, Neuberger MS. Immunoglobulin isotype switching is inhibited and somatic hypermutation perturbed in UNG-deficient mice. *Curr Biol*. 2002; 12:1748–55. [PubMed: 12401169]
- Rajewsky K. Clonal selection and learning in the antibody system. *Nature*. 1996; 381:751–8. [PubMed: 8657279]
- Ratnam S, Bozek G, Nicolae D, Storb U. The pattern of somatic hypermutation of Ig genes is altered when p53 is inactivated. *Mol Immunol*. 2010; 47:2611–8. [PubMed: 20691478]
- Roa S, Avdievich E, Peled JU, Maccarthy T, Werling U, Kuang FL, Kan R, Zhao C, Bergman A, Cohen PE, Edelmann W, Scharff MD. Ubiquitylated PCNA plays a role in somatic hypermutation and class-switch recombination and is required for meiotic progression. *Proc Natl Acad Sci U S A*. 2008; 105:16248–53. [PubMed: 18854411]
- Ross AL, Sale JE. The catalytic activity of REV1 is employed during immunoglobulin gene diversification in DT40. *Mol Immunol*. 2006; 43:1587–94. [PubMed: 16263170]
- Rush JS, Liu M, Odegard VH, Unniraman S, Schatz DG. Expression of activation-induced cytidine deaminase is regulated by cell division, providing a mechanistic basis for division-linked class switch recombination. *Proc Natl Acad Sci U S A*. 2005; 102:13242–7. [PubMed: 16141332]
- Schenten D, Kracker S, Esposito G, Franco S, Klein U, Murphy M, Alt FW, Rajewsky K. Pol zeta ablation in B cells impairs the germinal center reaction, class switch recombination, DNA break repair, and genome stability. *J Exp Med*. 2009; 206:477–90. [PubMed: 19204108]
- Schrader CE, Guikema JE, Wu X, Stavnezer J. The roles of APE1, APE2, DNA polymerase beta and mismatch repair in creating S region DNA breaks during antibody class switch. *Philos Trans R Soc Lond B Biol Sci*. 2009; 364:645–52. [PubMed: 19010771]
- Shen HM, Tanaka A, Bozek G, Nicolae D, Storb U. Somatic hypermutation and class switch recombination in Msh6(–/–)Ung(–/–) double-knockout mice. *J Immunol*. 2006; 177:5386–92. [PubMed: 17015724]

- Soria G, Podhajcer O, Prives C, Gottifredi V. P21Cip1/WAF1 downregulation is required for efficient PCNA ubiquitination after UV irradiation. *Oncogene*. 2006; 25:2829–38. [PubMed: 16407842]
- Soria G, Speroni J, Podhajcer OL, Prives C, Gottifredi V. p21 differentially regulates DNA replication and DNA-repair-associated processes after UV irradiation. *J Cell Sci*. 2008; 121:3271–82. [PubMed: 18782865]
- Stelter P, Ulrich HD. Control of spontaneous and damage-induced mutagenesis by SUMO and ubiquitin conjugation. *Nature*. 2003; 425:188–91. [PubMed: 12968183]
- Watanabe K, Tateishi S, Kawasuji M, Tsurimoto T, Inoue H, Yamaizumi M. Rad18 guides poleta to replication stalling sites through physical interaction and PCNA monoubiquitination. *Embo J*. 2004; 23:3886–96. [PubMed: 15359278]
- Wiesendanger M, Kneitz B, Edelmann W, Scharff MD. Somatic hypermutation in MutS homologue (MSH)3-, MSH6-, and MSH3/MSH6-deficient mice reveals a role for the MSH2-MSH6 heterodimer in modulating the base substitution pattern. *J Exp Med*. 2000; 191:579–84. [PubMed: 10662804]
- Wilson TM, Vaisman A, Martomo SA, Sullivan P, Lan L, Hanaoka F, Yasui A, Woodgate R, Gearhart PJ. MSH2-MSH6 stimulates DNA polymerase eta, suggesting a role for A:T mutations in antibody genes. *J Exp Med*. 2005; 201:637–45. [PubMed: 15710654]
- Woo M, Hakem R, Furlonger C, Hakem A, Duncan GS, Sasaki T, Bouchard D, Lu L, Wu GE, Paige CJ, Mak TW. Caspase-3 regulates cell cycle in B cells: a consequence of substrate specificity. *Nat Immunol*. 2003; 4:1016–22. [PubMed: 12970760]
- Zan H, Komori A, Li Z, Cerutti A, Schaffer A, Flajnik MF, Diaz M, Casali P. The translesion DNA polymerase zeta plays a major role in Ig and bcl-6 somatic hypermutation. *Immunity*. 2001; 14:643–53. [PubMed: 11371365]
- Zeng X, Winter DB, Kasmer C, Kraemer KH, Lehmann AR, Gearhart PJ. DNA polymerase eta is an A-T mutator in somatic hypermutation of immunoglobulin variable genes. *Nat Immunol*. 2001; 2:537–41. [PubMed: 11376341]

**Fig. 1.**

p21 expression is not regulated by AID. B cells were isolated from splenocytes and stimulated with LPS and IL-4 for the time periods indicated. Relative p21 mRNA expression was determined after normalizing to β -actin. Fold-differences are shown by setting the p21 expression level at time 0 hr to one. There are no significant differences in p21 expression between AID-sufficient (*Aicda*^{+/+}) and AID-deficient (*Aicda*^{-/-}) B cells at all time periods as indicated by two-tailed unpaired Student's *t*-tests, $p \geq 0.1$. Comparison of p21 expression between each time point was only statistically different between time points 0, 8, and 24 hours ($p = 3.6 \times 10^{-5}$ comparing time 0hr with 8hr, $p = 0.006$ comparing time 0hr with 24hr, $p = 0.0015$ comparing time 24hr with 48hr). The *p* values between 48hr and 72hr was 0.6, and the *p* value between time 48hr and 96hr was 0.09. *P* values were determined by two-tailed unpaired Student's *t*-tests. Three independent experiments were performed from 3 *Aicda*^{-/-} and 2 *Aicda*^{+/+} mice. Error bars represent standard deviations (SD).

**Fig. 2.**

p21 is dispensable for SHM. (A) Top: SHM frequency was determined from activated B cells that were isolated from Peyer's patches and the Jh2-Jh4 intronic region was amplified. Three independent experiments (4 mice per genotype per experiment) were performed. Mutation frequency was determined by dividing the total number of mutations to the number of total bp analyzed. Error bars represent standard deviations (SD). *P* values calculated using two-tailed unpaired Student's *t*-tests. Bottom: Pie charts representing data for SHM. The center of the pie indicates the number of clones sequenced. The numbers around the pie chart represent the number of mutations. The numbers inside the parenthesis are the percentages of clones containing the indicated number of mutations. (B) SHM spectrum. Total number of mutations from three independent experiments are represented in the tables on the right whereas the tables on the left indicate the percentages of mutations at each bp. (C) To simplify the comparison of mutation patterns, the SHM frequency at each bp, corrected for base composition, is shown. The results were confirmed by the SHMTool webserver program (<http://scb.aecom.yu.edu/cgi-bin/p1>). There were no statistical differences found by two-tailed unpaired Student's *t*-tests. Error bars represent SD.

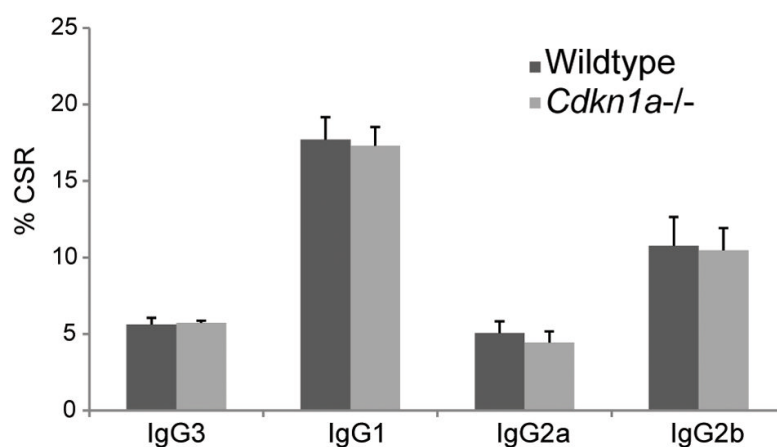


Fig. 3. p21 deficiency does not affect CSR to IgG1, IgG3, IgG2a, and IgG2b. B cells from *Cdkn1a*^{-/-} and *Cdkn1a*^{+/+} mice were stimulated with the appropriate cytokines (see materials and methods) for 4 days to induce CSR. The percentage of cells that switched to the indicated isotypes were determined by flow cytometry. Three independent experiments (1 mouse per genotype per experiment) were performed. Error bars represent SD.

Table 1

SHM summary (Jh2-Jh4 Peyer's Patches)

	Wildtype	<i>Cdkn1a</i> ^{-/-}	<i>p</i> value
Total number of base pairs analyzed ^a	171,580	147,708	
Total number of mutations ^b	524	383	
Overall mutation frequency ^c	3.21×10^{-3}	2.77×10^{-3}	0.44
Mutated sequences (%)	56.0	54.0	
Total transition mutations (%)	51.3	49.9	0.27
Total transversion mutations (%)	48.7	50.1	0.54
A/T mutations (%)	62.8	61.9	0.58
% Transitions	30.2	27.2	0.24
% Transversions	32.6	34.7	0.59
G/C mutations (%)	37.2	38.1	0.58
% Transitions	21.2	22.7	0.70
% Transversions	16.0	15.4	0.84
AID hotspots (%) ^d			
W <u>C</u> /	8.8	10.2	0.55
/ <u>G</u> YW	8.4	11.0	0.06
Pol η hotspots (%) ^d			
W <u>A</u> /	31.5	26.4	0.29
/ <u>T</u> W	12.4	12.8	0.99

^a 1.4 kb Jh2-Jh4 intronic region was amplified from activated B cells and sequenced bidirectionally. Three independent experiments (4 mice per genotype per experiment) were performed.

^b Clones containing the same mutations were counted once.

^c Mutation frequency was calculated by dividing the total number of mutations by the total number of base pairs analyzed. The results were confirmed by using the SHMTool webserver (<http://scb.aecom.yu.edu/cgi-bin/p1>).

^d Underlined site of the motif is scored. W = A/T, R = A/G, Y = C/T. Motifs were identified using SHMTool webserver.